PECULIARITIES OF PHASE EQUILIBRIA IN THE Li-Mn-Eu-O SYSTEM INVOLVING MELT

Grigorii BUZANOV, George NIPAN, Konstantin ZHIZHIN

Kurnakov Institute of General and Inorganic Chemistry of the RAS
31 Leninskiy prospect, Moscow 119991, Russia, e-mail: gbuzanov@yandex.ru

Solution of a multifaceted problem of effective materials production, along with the development of methods for the synthesis of required chemical and phase composition substances, must ensure the reproducibility of specified functional properties (electrochemical, magnetic etc.) of the materials. In the case of a real multicomponent material with different volatility of the components it consists of, slight temperature or pressure fluctuations of the volatile component during synthesis procedure can cause a considerable effect on the elemental and phase composition of the matter, and hence affect its physicochemical (and functional) properties. Deviations from the initial composition can also occur under the operating conditions of this material, which is especially important for systems where one of the components is a transition (TM) or rare earth metal (REM) with several stable oxidation states. Thus, the solution of this complex problem should include the study of phase equilibria (both stable and metastable) in a given multicomponent system in a wide range of temperature, concentrations of components, and partial pressure of the volatile component(s).

A good example of such a system is the Li-Mn-Eu-O system, crystalline materials of which are of significant technological interest (cathodes for Li-ion batteries, magnetic, including spintronic materials etc). Currently, no systematic study of Li-TM-REM-O systems has been carried out. The ternary system Li-Mn-O was the object of study in a number of research [1]. Of the Li-REE-O systems, the only example for which a detailed plot of phase equilibria exists today is Li-Eu-O [2].

EXPERIMENTAL SECTION

Reaction apparatus

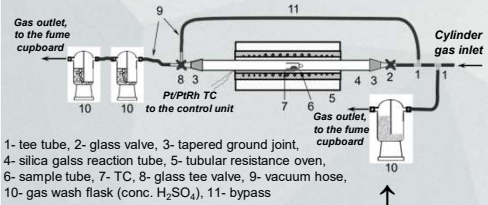

1- tee tube, 2- glass valve, 3- tapered ground joint, 4- silica gass reaction tube, 5- tubular resistance oven, 6- sample tube, 7- TC, 8- glass tee valve, 9- vacuum hose, 10- gas wash flask (conc. H_2SO_4), 11- bypass

Air: RT ÷ 1473 K (muffle furnace)
Ar, O_2, H_2 etc.: RT ÷ 1273 K (tubular furnace)

Controlled gas media for syntheses

Gas media	Patrial pressure P(X), atm
Air	$P(O_2) \approx 0.21$
Oxygen "4.0"	$P(O_2) \approx 1$
Argon "5.5", 99.9995% Ar	$P(O_2) \approx 0,0001$
Hydrogen "6.0", 99.9999% H_2	$P(H_2) \approx 1$
Argon+5% (vol.) H_2	$P(H_2) \approx 0.05$

Precursors & Mechanochemical treatment

Li_2CO_3, β-MnO_2, β-Mn_2O_3, Eu_2O_3 (99,98%), $LiOH{\cdot}H_2O$ (99%), $LiNO_3{\cdot}3H_2O$ (99,9%), LiH (98%, H_2 gas volumetric), Eu (99%), Mn (99,5%), Li (99,6%)

Rersch MM400 vibromill, grinding jars & balls (steel, ZrO_2)
Typical conditions of ball milling (BM): 30 min, 30 Hz, ball to specimen mass ratio ≈ 20 : 1

Solid-state synthesis scheme

Starting reagents: mixtures of binary/ternary compds with preset Li : Mn : Eu ratio

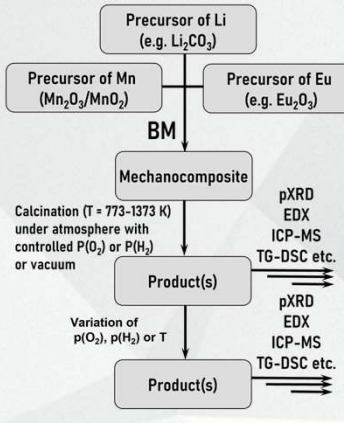

Simplified mechanocomposite model

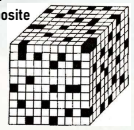

Activated domains of precursors

RESULTS: TERNARY SYSTEMS

Mn-Eu-O SYSTEM

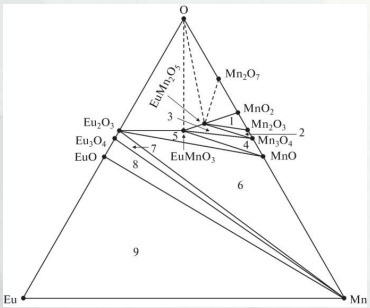

Fig. 1: Subsolidus equilibria in the Eu–Mn–O system (x–y–projection of the P–T–x–y–phase diagram)

We used experimental and literature data to plot x–y and P_{O2}–T projections of the P–T–x–y diagram of the Eu–Mn–O system (Figs. 1 and 2), where there are imaged subsolidus phase equilibria involving three crystalline phases and oxygen. The solid lines on the projections are experimental, and dashed lines are hypothetical. $EuMn_2O_5$–MnO_2–Mn_2O_7–O_2 monovariant equilibrium (Fig. 1) is not considered on the P_{O2}–T projection because of the low melting temperature of Mn_2O_7 (~280 K). The dashed tie-lines $EuMnO_3$–O and $EuMn_2O_5$–O on Fig. 5 are drawn formally to demarcate the triangles corresponding to divariant equilibria $EuMn_2O_5$–Mn_2O_7–O_2, $EuMnO_3$–$EuMn_2O_5$–O_2, and Eu_2O_3–$EuMnO_3$–O_2. The suggestion about the existence of monovariant equilibrium Eu_2O_3–$EuMnO_3$–$EuMn_2O_5$–O_2 is not verified experimentally [9]; however, this is at variance with the results of our work (Fig. 2, curve c) and can arise from the differing total compositions of the samples; tie-line Eu_2O_3–$EuMn_2O_5$ is absent on the x–y projection. [3]

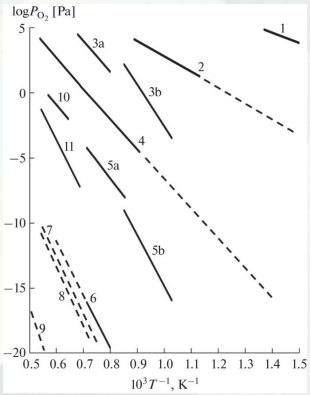

P_{O_2}–T projection of the P–T–x–y phase diagram of the Eu–Mn–O system

Li-Eu-O SYSTEM

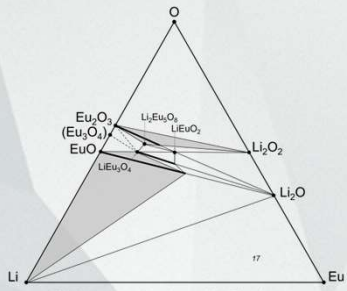

Fig.3: x-y-projection of Li-Eu-O system

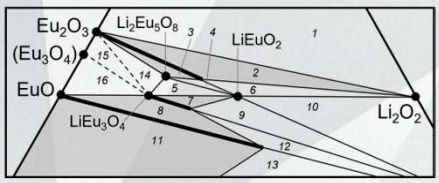

Fig.4: Fragment of the x-y-projection, demonstrating phase equilibria involving solid solutions based on EuO, Eu_2O_3 and $LiEu_3O_4$

The solubility of lithium in EuO_y one of the most promising spintronics materials, has been estimated for the first time (as well as it's cubic lattice contraction), which is at least 50–60%, and that for Eu_2O_3 and $LiEu_3O_4$ is 30% of the total amount of cations. Along with $LiEuO_2$, the formation of crystalline mixed-valent (simultaneously Eu^{II}+Eu^{III}) phases $LiEu_3O_4$ and $Li_2Eu_5O_8$ was confirmed. Using own experimental data, the x-y-projection of Li-Eu-O system were plotted (**Fig. 3**). Phase equilibria involving solid solutions is shown on **Fig. 4.** Two-phase equilibria regions: **1**– Li_2O–Eu_2O_3, **2**– *ss*Eu_2O_3–Li_2O_2, **3**– *ss*Eu_2O_3–$Li_2Eu_5O_8$, **7**– $LiEuO_2$–*ss*$LiEu_3O_4$, **8**– *ss*EuO–*ss*$LiEu_3O_4$, **11**– *ss*EuO–Li, three-phase equilibria regions: **4**– $LiEuO_2$–*ss*Eu_2O_3–$Li_2Eu_5O_8$, **5**– $LiEu_3O_4$–$LiEuO_2$–$Li_2Eu_5O_8$, **6**– *ss*Eu_2O_3–$LiEuO_2$–Li_2O_2, **9**– $LiEuO_2$–Li_2O–*ss*$LiEu_3O_4$, **10**– $LiEuO_2$–Li_2O_2–Li_2O, **12**– Li_2O–*ss*EuO–*ss*$LiEu_3O_4$, **13**– Li–Li_2O–*ss*EuO, **17**- Li–Li_2O–Eu. Equilibria **14** (Eu_2O_3–$Li_2Eu_5O_8$–$LiEu_3O_4$), as well as the ones involving Eu_3O_4 phase-**15** (Eu_2O_3–Eu_3O_4–$LiEu_3O_4$) and **16** (Eu_3O_4–EuO–$LiEu_3O_4$) are hypothetical, because applying the LiH as reducing agent the presence of Eu_3O_4 in equilibria were not observed, that can be explained with the formation of ternary $Li_2Eu_5O_8$ and $LiEu_3O_4$ compounds.

QUATERNARY SYSTEM Li-Mn-Eu-O

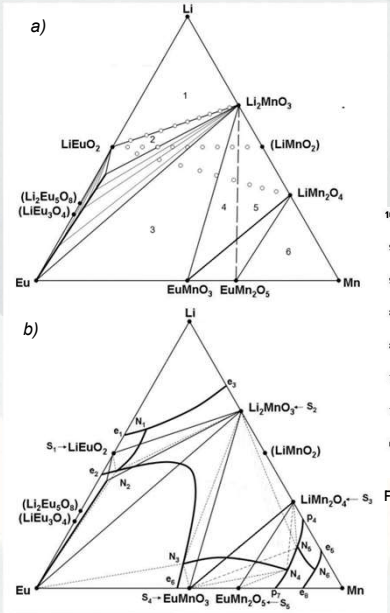

Fig.5: a – subsolidus equilibria (p-T-x-y-projection), ○- experimental compounds, b – projection of the liquidus surface

For experimental study the quaternary system Li–Mn–Eu–O have been sectionized into three quasibinary sections: $LiEuO_2$-Li_2MnO_3 section ($Li_{1+x}Eu_{1-x}Mn_xO_{3-\delta}$ series), $LiEuO_2$-$LiMnO_2$ section ($LiEu_{1-x}Mn_xO_{2-\varepsilon}$ series) and $LiEuO_2$-$LiMn_2O_4$ ($LiEu_{1-x}Mn_{2x}O_{4-\gamma}$ series), $0 \le x < 1$, $\Delta x = 0.1$. Based on the pXRD and TG-DSC (in air) data for the temperature range of RT-1100 °C, the subsolidus equilibria (p-T-x-y-projection, **Fig 5a**), projection of the liquidus surface (**Fig. 5b**), as well as polythermal diagrams of the Li_2O–Eu_2O_3–$Mn_2O_3(Mn_3O_4)$ (**Fig. 6 a,b**). Areas 1-6 (Fig. 5a) correspond to ternary equilibria 1- L_2O–Li_2MnO_3–$LiEuO_2$, 2-Li_2MnO_3–$LiEuO_2$–*ss*Eu_2O_3, 3- Li_2MnO_3–*ss*Eu_2O_3–$EuMnO_3$, 4- Li2MnO_3–$EuMnO_3$–$EuMn_2O_5$, 5- Li_2MnO_3–$EuMn_2O_5$–$LiMn_2O_4$ и 6- $EuMn_2O_5$–$LiMn_2O_4$–Mn_2O_3 (Mn_3O_4). No formation of novel quaternary phases, except solid solutions based on spinel phase $LiMn_2O_4$ (2% Eu solubility, $LiMn_{0.98}Eu_{0.02}O_{4-\delta}$) have been detected. $LiMnO_2$, $LiEu_3O_4$ and $Li_2Eu_5O_8$ are not being formed in air ($P(O_2)$ = 0.21 atm), not found in equilibria and hence placed in brackets at the corresponding plots (**Fig. 5 a,b**).

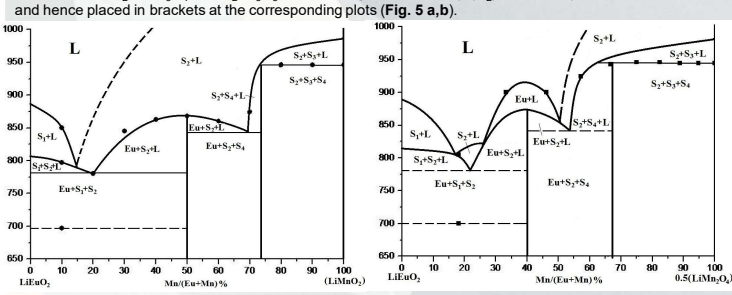

Fig.6: polythermal diagrams of the Li_2O–Eu_2O_3–$Mn_2O_3(Mn_3O_4)$ system: (a) $LiEuO_2$–$LiMnO_2$ cross section, (b) $LiEuO_2$–$LiMn_2O_4$ section

Eu_2O_3, $LiEuO_2$, Li_2MnO_3, $LiMn_2O_4$, $EuMnO_3$, $EuMn_2O_5$ and melt are marked as Eu, S1, S2, S3, S4, S5 and L. Eutectic (e) and peritectic (p) equilibria of binary systems are marked on the sides of the triangle (**Fig. 5b**): $e_1(S_{Li2O}+L+S_1)$, $e_2(S_{Eu2O3}+L+S_1)$, $e_3(S_{Li2O}+L+S_2)$, $p_4(S_2+S_3+L)$, $e_5(S_3+L+S_{Mn2O3})$, $e_6(S_{Eu2O3}+L+S_4)$, $p_7(S_4+S_5+L)$, and $e_8(S_5+L+S_{Mn2O3})$.

[1] Buzanov G.A., Nipan G.D. et al. doi:10.1134/s0036023617050059
[2] Buzanov G.A., Nipan G.D., RJIC, 2023, accepted manuscript
[3] Buzanov G.A., Nipan G.D. doi: 10.1134/S0036023622070051

This work was financially supported by Russian Science Foundation (project 23-23-00576)
XVI Chinese-Russian Symposium "Novel Materials and Technologies"
05-14.10.2023, Haikou, PRC